

Supporting Information (SI)

# Grain Boundaries Modified Uniformly-Conjoint Metal/Oxides via Binder Strategy as Efficient Bifunctional Electrocatalysts

*Rongrong Zhang, Li Wang, Yu-Hang Ma, Lun Pan,\* Ruijie Gao, Ke Li, Xiangwen Zhang, Ji-Jun Zou*

Key Laboratory for Green Chemical Technology of the Ministry of Education, School of Chemical Engineering and Technology, Tianjin University, Tianjin 300072, China.

Collaborative Innovative Center of Chemical Science and Engineering (Tianjin), Tianjin 300072, China.

Corresponding author email address:

E-mail: panlun76@tju.edu.cn (L. Pan)

# Table of contents

	<b>Captions</b>	<b>Page</b>
<b>Figure S1</b>	XRD of CoNim-Gly and CoNi-Gly.	<b>S3</b>
<b>Figure S2</b>	Schematic of melamine lie in interlamination of glyceric metal precursor (CoNim-Gly).	<b>S3</b>
<b>Figure S3</b>	IR of CoNim-Gly and CoNi-Gly.	<b>S4</b>
<b>Figure S4</b>	TG and DTG in argon flow of CoNim-Gly and CoNi-Gly.	<b>S4</b>
<b>Figure S5</b>	TEM of CoNi.	<b>S5</b>
<b>Figure S6</b>	HRTEM of CoNi.	<b>S5</b>
<b>Figure S7</b>	TEM of CoNi-melamine with different Co/Ni ratio. Com and Nim are synthesized with only one metal source of cobalt and nickel respectively.	<b>S5</b>
<b>Figure S8</b>	XRD of CoNim and CoNi.	<b>S6</b>
<b>Figure S9</b>	The linear combination fitting (LCF) of XANES for CoNi which main component is metal.	<b>S6</b>
<b>Figure S10</b>	The fine X-ray photoelectron spectroscopy (XPS) of CoNi and CoNim, fitting of O 1s.	<b>S7</b>
<b>Table S1</b>	Elements concentration of CoNim and CoNi by XPS.	<b>S8</b>
<b>Figure S11</b>	The XANES of Co K-edge for CoNim.	<b>S9</b>
<b>Figure S12</b>	The XANES of Ni K-edge for CoNim.	<b>S9</b>
<b>Figure S13</b>	XRD of Com and Nim.	<b>S10</b>
<b>Figure S14</b>	RRDE tests for electron transfer number of Pt/C (a), IrO <sub>2</sub> (b), and RuO <sub>2</sub> (c).	<b>S11</b>
<b>Figure S15</b>	LSV of IrO <sub>2</sub> (a) and RuO <sub>2</sub> (b) before and after 2000 cycle tests.	<b>S12</b>
<b>Figure S16</b>	HRTEM of CoNim after OER stability test (washed from electrode).	<b>S13</b>
<b>Figure S17</b>	HRTEM of CoNim after ORR stability test (washed from electrode)	<b>S13</b>
<b>Figure S18</b>	Optimized adsorption structures of metal and metal oxides with (100) crystal faces.	<b>S14</b>
<b>Figure S19</b>	Optimized OH adsorption structures of (100) crystal faces with composite clusters.	<b>S15</b>
<b>Figure S20</b>	Optimized O <sub>2</sub> adsorption structures of (100) crystal faces with composite clusters.	<b>S16</b>
<b>Figure S21</b>	Galvanostatic (10 mA/cm <sup>2</sup> ) charge-discharge cycling curves for Pt/C-IrO <sub>2</sub> (a) and CoNim (b).	<b>S17</b>
<b>Figure S22</b>	(a,b) Co 2p and Ni 2p XPS spectra of CoNim surface after OER stability test. In Co 2p and Ni 2p XPS, the surface Co, Co <sup>2+</sup> and Ni, Ni <sup>2+</sup> were oxidized to Co <sup>3+</sup> and Ni <sup>3+</sup> .	<b>S18</b>
//	<i>XAFS fit specific information.</i>	<b>S19</b>
//	<i>References</i>	<b>S20</b>

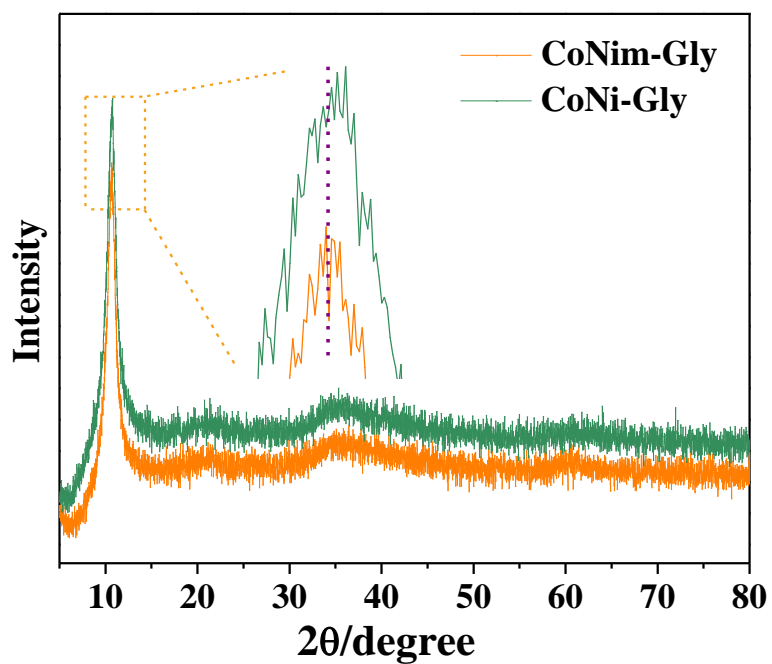


Figure S1. XRD of CoNim-Gly and CoNi-Gly.

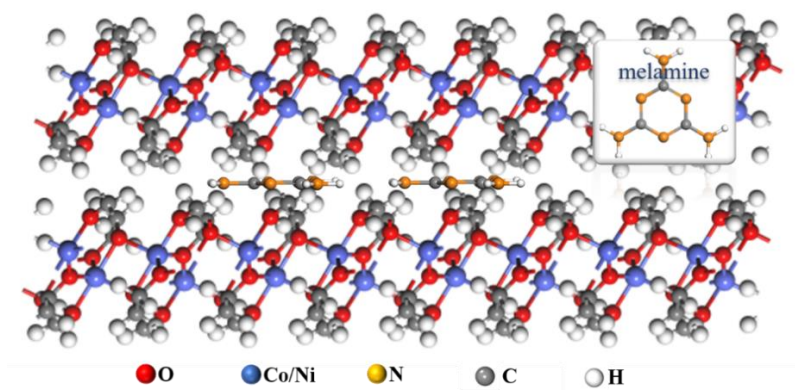
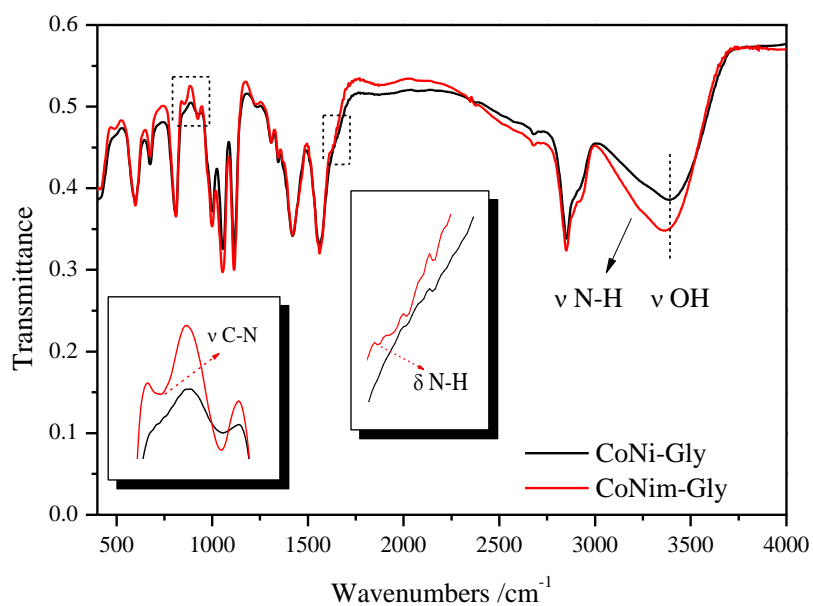
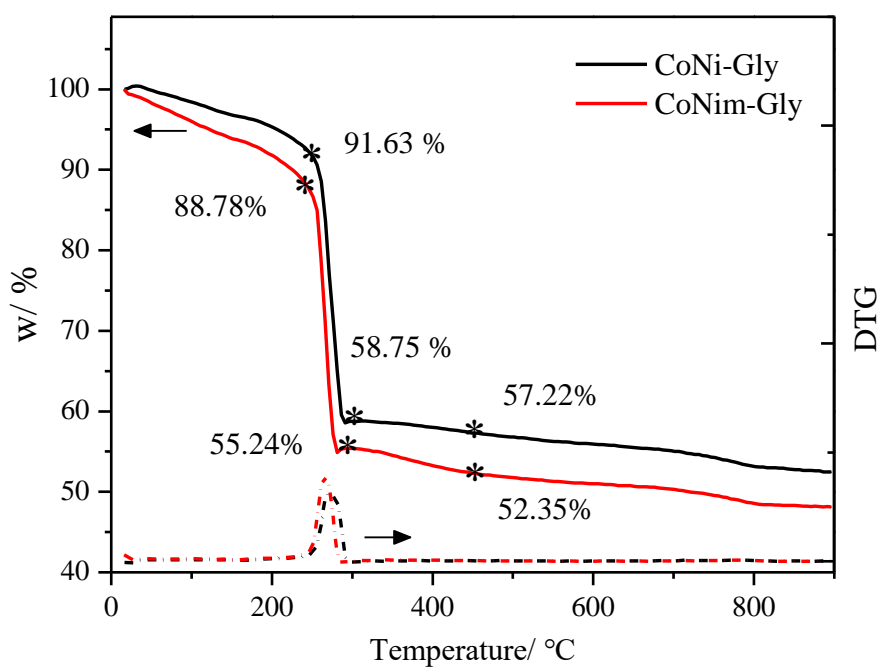


Figure S2. Schematic of melamine lie in interlamination of glyceric metal precursor (CoNim-Gly).



**Figure S3.** IR of CoNim-Gly and CoNi-Gly.



**Figure S4.** TG and DTG in argon flow of CoNim-Gly and CoNi-Gly.

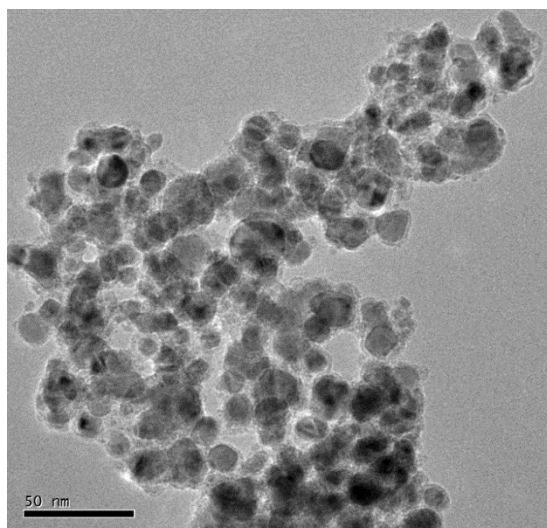


**Figure S5.** TEM of CoNi.

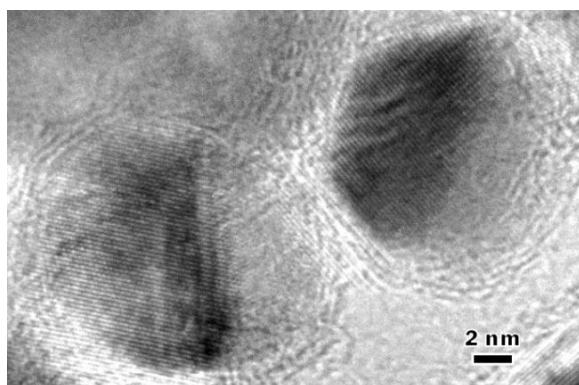


**Figure S6.** HRTEM of CoNi.

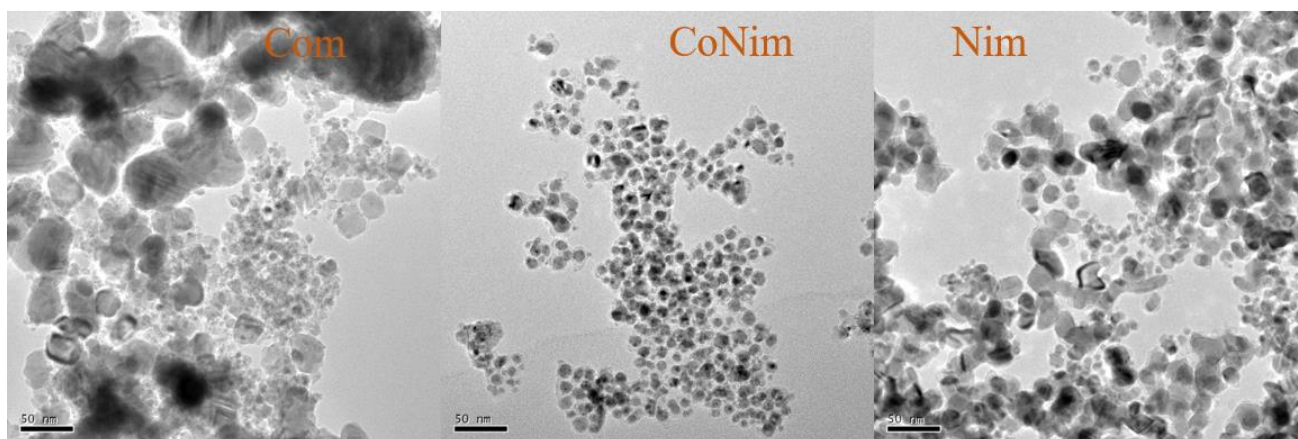


**Figure S7.** TEM of CoNi-melamine with different Co/Ni ratio. Com and Nim are synthesized with only one metal source of cobalt and nickel respectively.

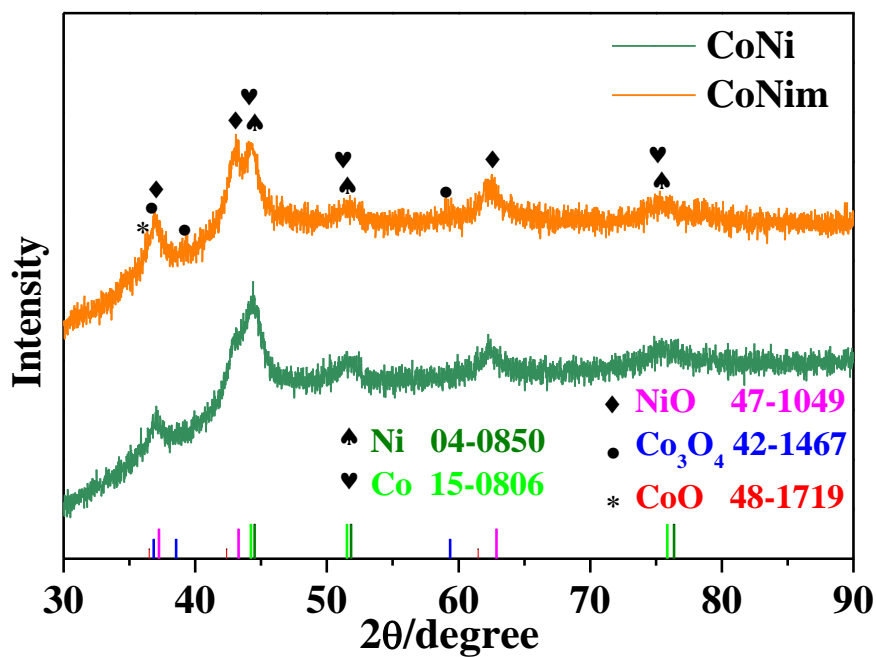


Figure S8. XRD of CoNim and CoNi.

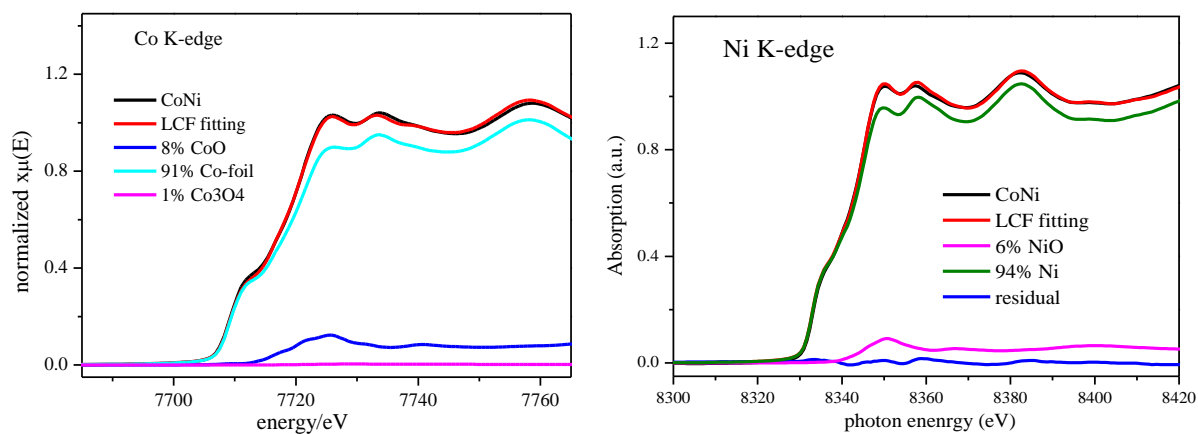
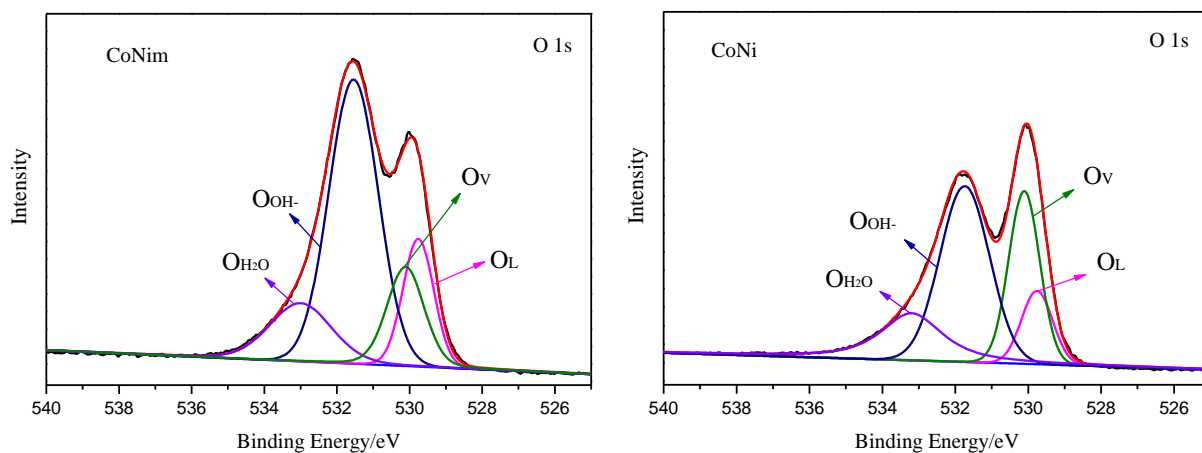


Figure S9. The linear combination fitting (LCF) of XANES for CoNi which main component is metal.



**Figure S10.** The fine X-ray photoelectron spectroscopy (XPS) of CoNi and CoNiM, fitting of O 1s. O<sub>L</sub> is oxygen-metal in lattice, O<sub>v</sub> is oxygen-metal in edge and interface, OOH<sub>-</sub> and OH<sub>2</sub>O are adsorbed oxygen from air.<sup>1</sup> Using lattice oxygen atoms (O<sub>L</sub> and O<sub>v</sub>) represent oxides content according to these fittings.

**Table S1.** Elements concentration of CoNim and CoNi by XPS.

Name	CoNim	CoNi
C	45.53	49.90
O	35.43	26.71
Co	10.30	11.27
Ni	8.74	12.12



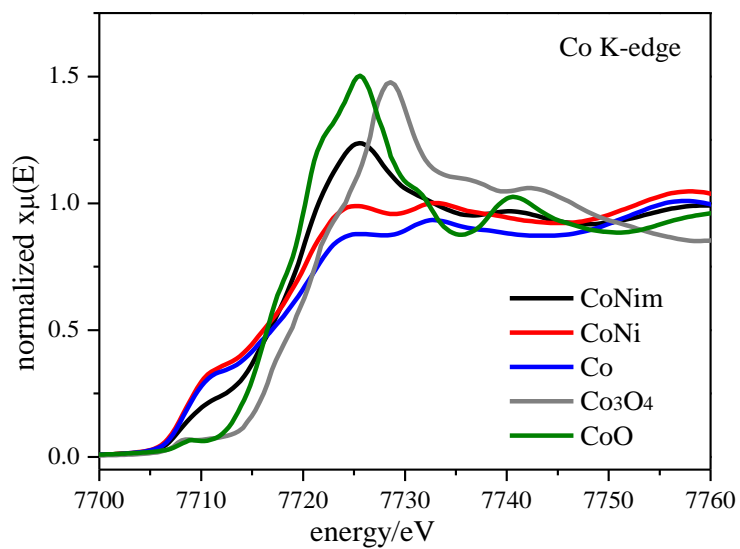


**Figure S11.** The XANES of Co K-edge for CoNim.

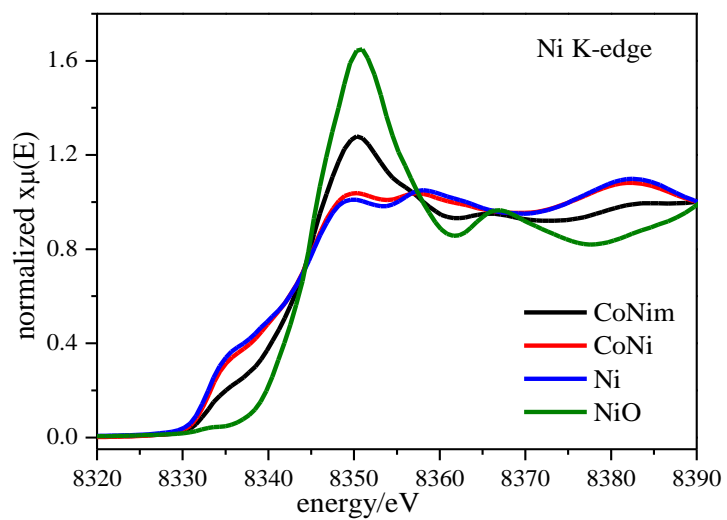


**Figure S12.** The XANES of Ni K-edge for CoNim.

*Information of different Co/Ni ratio samples*

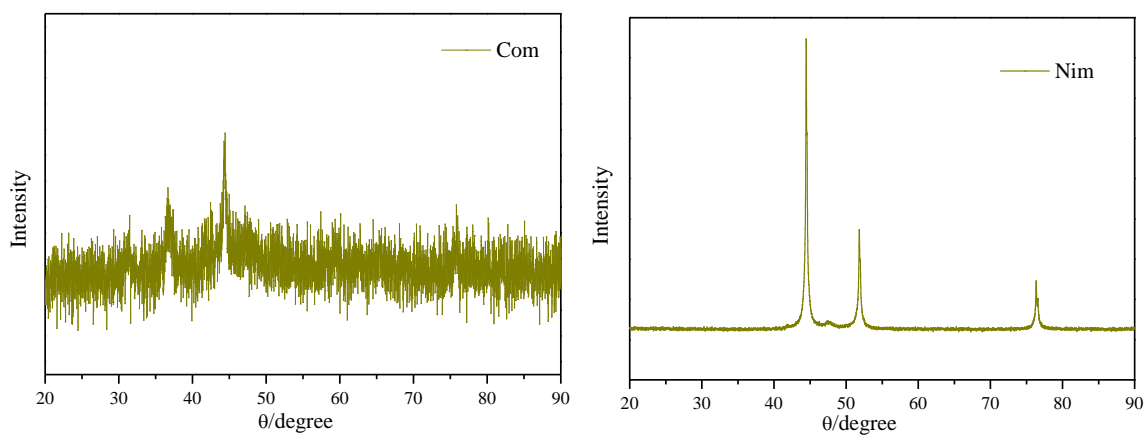


**Figure S13.** XRD of Com and Nim.

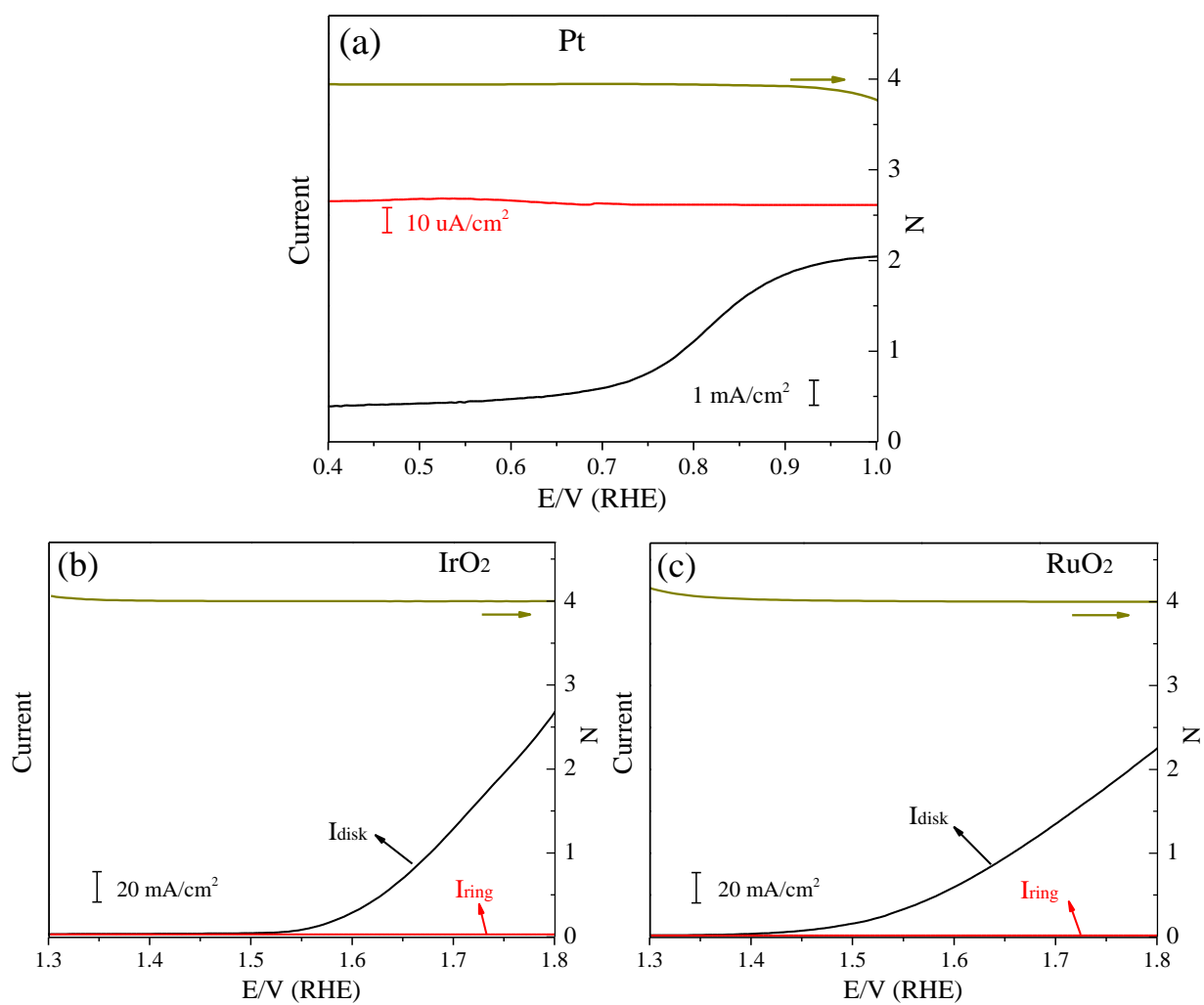


**Figure S14.** RRDE tests for electron transfer number of Pt/C (a), IrO<sub>2</sub> (b), and RuO<sub>2</sub> (c).

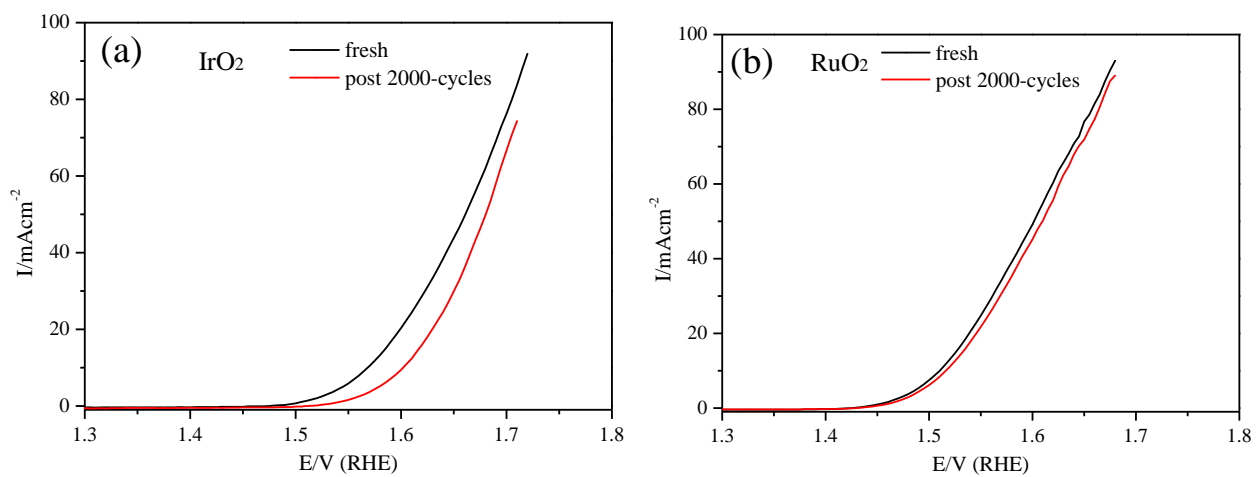


**Figure S15.** LSV of IrO<sub>2</sub> (a) and RuO<sub>2</sub> (b) before and after 2000 cycle tests.

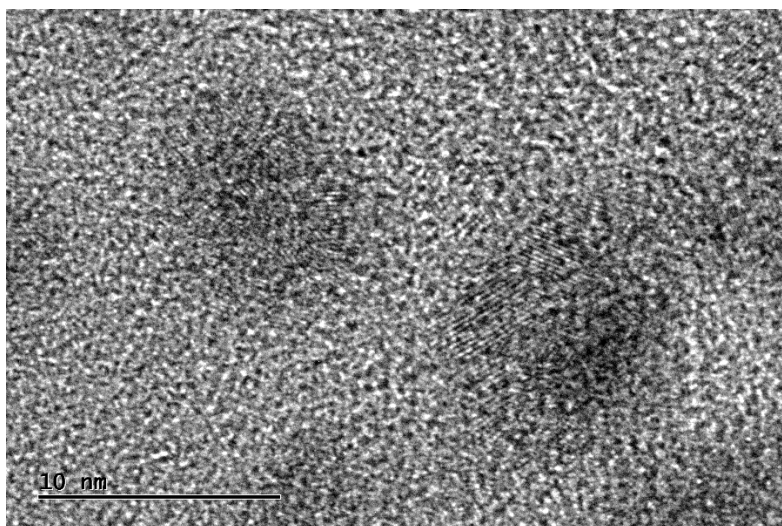


**Figure S16.** HRTEM of CoNim after OER stability test (washed from electrode).

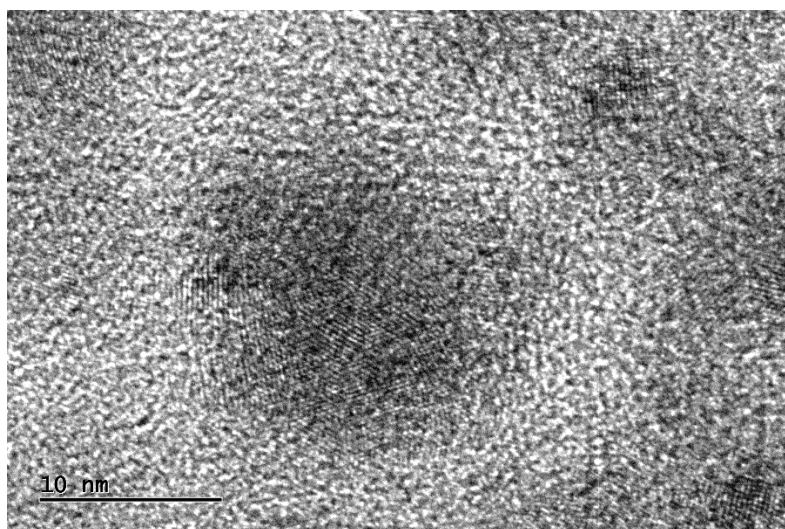


**Figure S17.** HRTEM of CoNim after ORR stability test (washed from electrode).

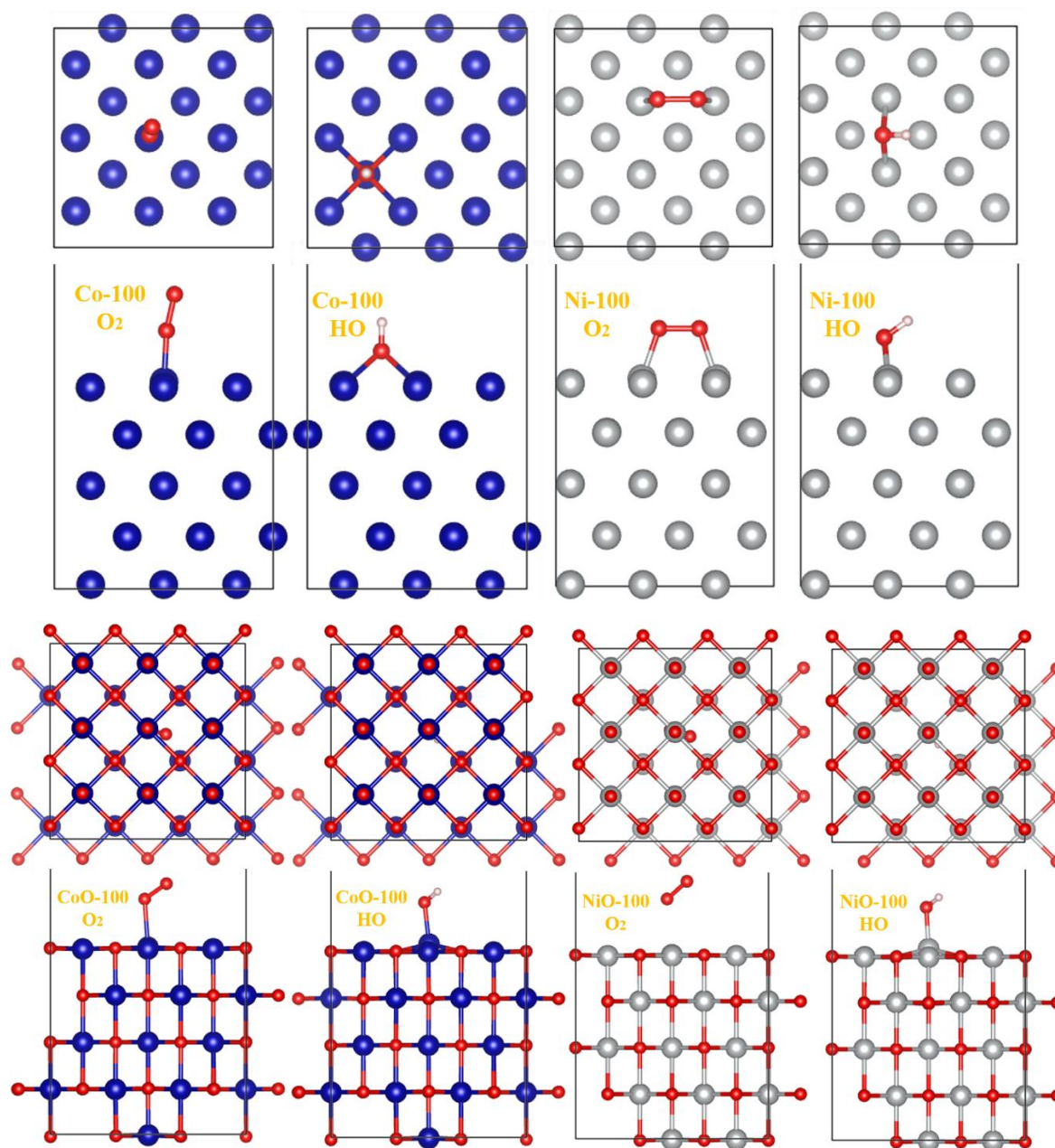


**Figure S18.** Optimized adsorption structures of metal and metal oxides with (100) crystal faces.

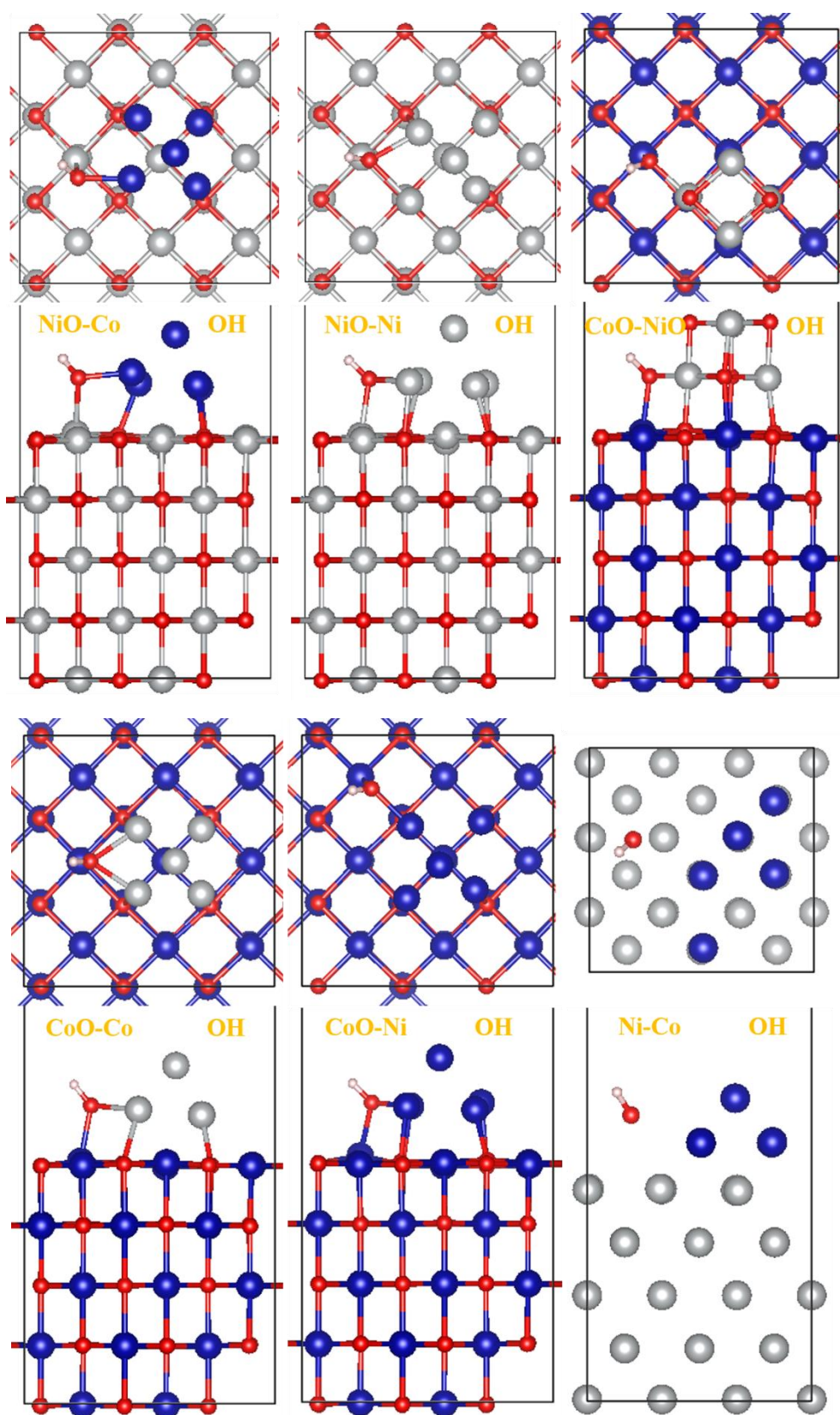


**Figure S19.** Optimized OH adsorption structures of (100) crystal faces with composite clusters.



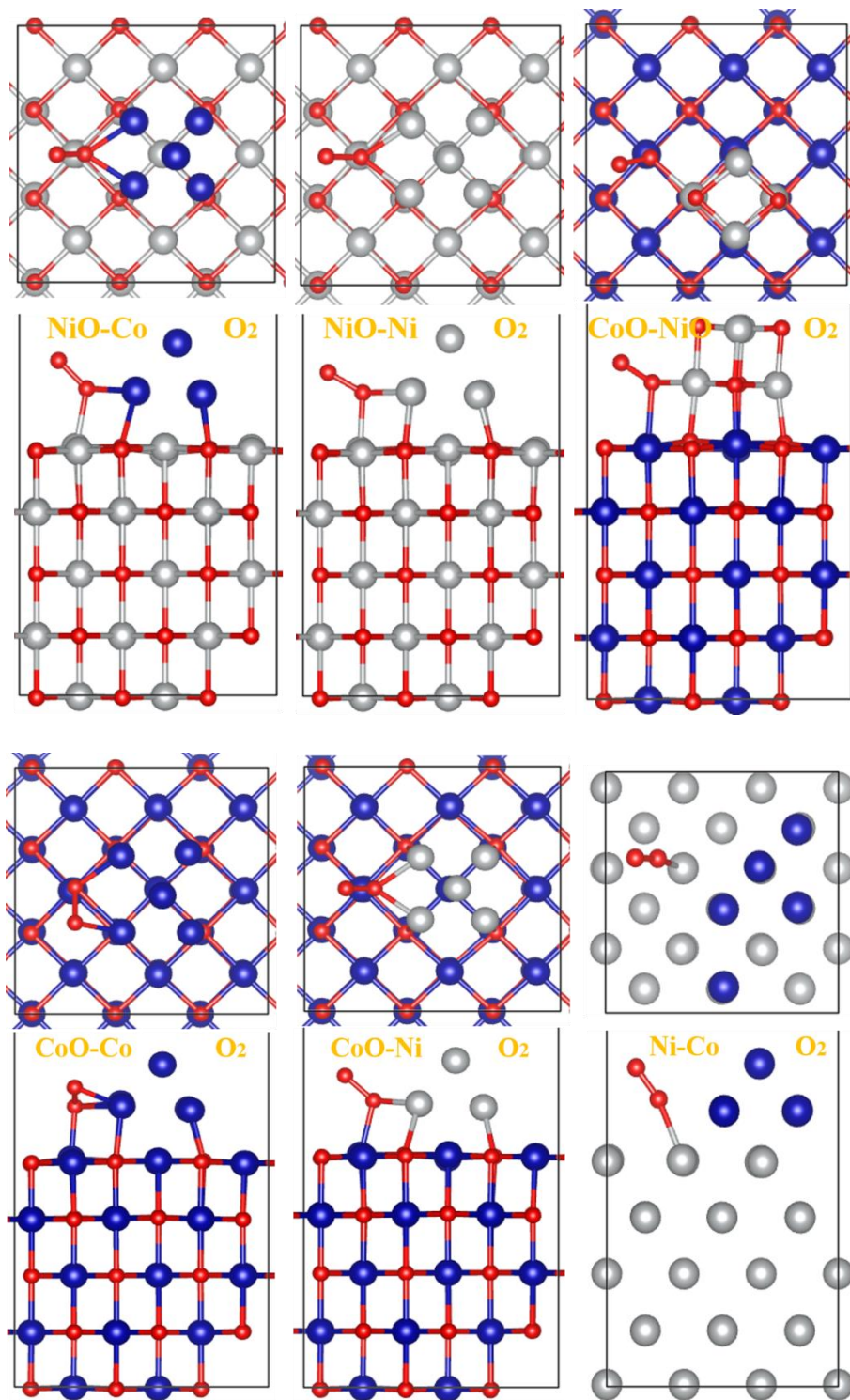


**Figure S20.** Optimized  $O_2$  adsorption structures of (100) crystal faces with composite clusters.



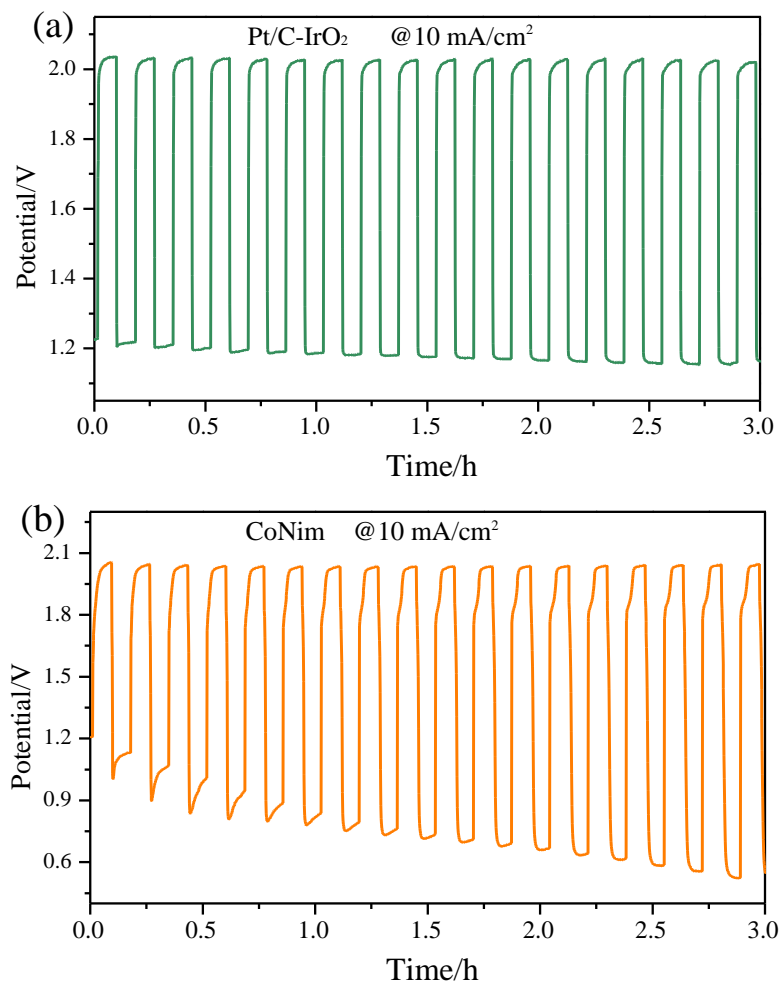


**Figure S21.** Galvanostatic (at 10 mA/cm<sup>2</sup>) charge-discharge cycling curves for Pt/C-IrO<sub>2</sub> (a) and CoNim (b).

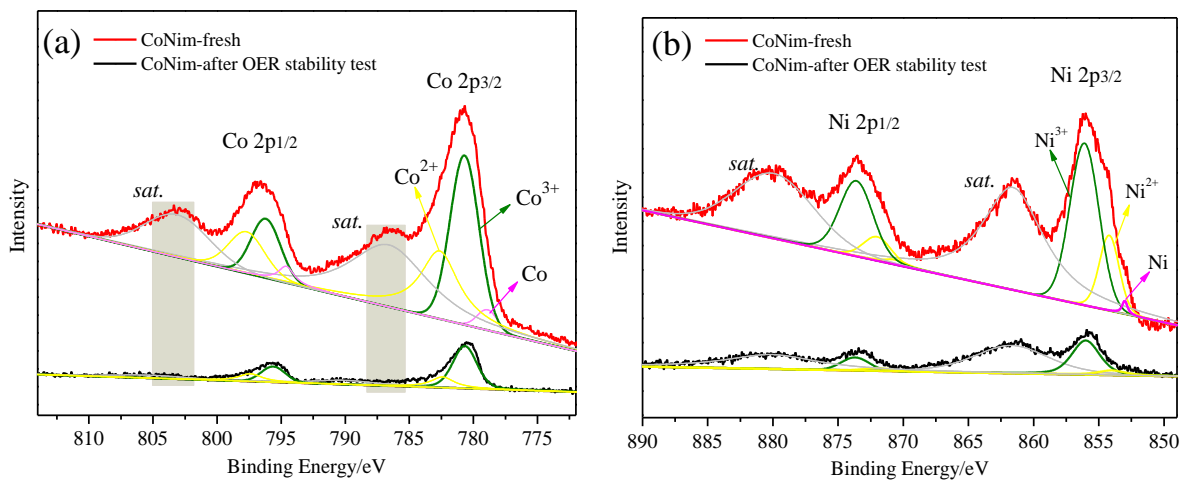


**Figure S22.** (a,b) Co 2p and Ni 2p XPS spectra of CoNim surface after OER stability test. In Co 2p and Ni 2p XPS, the surface Co, Co<sup>2+</sup> and Ni, Ni<sup>2+</sup> were oxidized to Co<sup>3+</sup> and Ni<sup>3+</sup>.

### ***XAFS fit specific information.***

Three paths from 1.10 Å to 2.85 Å (Co-O of Co<sub>3</sub>O<sub>4</sub>, Co-O of CoO, and Co-Co of Co metal) were used in Co k-edge adsorption spectrum fit, and three paths from 1.25 Å to 3.00 Å (Ni-O of NiO, Ni-Ni of Ni metal, Ni-Ni of NiO) were used in Ni k-edge adsorption spectrum fit. According to the principle and results of LCF, the following standard EXAFS formula can be used in absorption spectrum of mixed substances:

$$\chi(k) = \sum_j \frac{N_j S_0^2 f_j(k)}{k R_j^2} e^{-2k^2 \sigma_j^2} e^{-2R_j/\lambda_j(k)} \sin[2kR_j + \delta_j(k) + 2\varphi_C(k)]$$

$j=1, 2, 3$  represent three paths mentioned above.  $N_j$  denotes the total number of atoms in the  $j$ -th shell.  $S_0^2$  is the amplitude reduction factor.  $R$  is the distance between the absorbing and scattering atoms.  $\lambda(k)$  is the mean free path of the excited photoelectron.  $f(k)$  and  $\delta(k)$  are the backscattering amplitude and scattering phase shift of the scattering atom, respectively.  $\varphi_C(k)$  is phase-shift of the absorbing atom.  $\sigma^2$  known as the Debye-Waller factor, is the mean square variation in the interatomic distance  $R$  and  $e^{-2k^2 \sigma_j^2}$  term accounts for the effects of dynamic (thermal) vibration and configuration (structural) disorder which smear out the EXAFS oscillations at high  $k$  region. The  $N$  values obtained by fitting are multiplied by the ratio of the substance from LCF to obtain the atomic coordination number of each substance in the mixture.<sup>2</sup>

## Reference

1. Xu, L.; Jiang, Q.; Xiao, Z.; Li, X.; Huo, J.; Wang, S.; Dai, L., Plasma-Engraved  $\text{Co}_3\text{O}_4$  Nanosheets with Oxygen Vacancies and High Surface Area for the Oxygen Evolution Reaction. *Angew. Chem. Int. Ed.* **2016**, 55 (17), 5277-81.
2. Sun, Z.; Yan, W.; Yao, T.; Liu, Q.; Xie, Y.; Wei, S. XAFS in Dilute Magnetic Semiconductors. *Dalton T.* **2013**, 42, 13779-13801.